

RESEARCH ARTICLE

Article No: 24

Characteristics of Brain Metastases Identified by PET-CT Imaging in Patients with Lung Cancer

Çetin YAKIŞIK¹, Celal SATICI¹, Sinem Nedime SÖKÜCÜ¹, Ayşegül ERİNÇ¹, Reşit AKYEL², Şenay AYDIN³¹University of Health Sciences, Yedikule Chest Diseases and Thoracic Surgery Training and Research Hospital, Department of Pulmonology, İstanbul, Türkiye²University of Health Sciences, Yedikule Chest Diseases and Thoracic Surgery Training and Research Hospital, Department of Nuclear Medicine, İstanbul, Türkiye³University of Health Sciences, Yedikule Chest Diseases and Thoracic Surgery Training and Research Hospital, Department of Neurology, İstanbul, Türkiye

ABSTRACT

Introduction: Contrast enhanced magnetic resonance imaging (MRI) could not be performed in all patients due to some contraindications. We aimed to demonstrate the characteristics of brain metastases that could be diagnosed with positron emission tomography - computed tomography (PET-CT) among patients with lung cancer.

Methods: Four hundred thirty nine patients diagnosed with lung cancer and brain metastasis between 2019 and 2023 were evaluated. A total of 642 brain metastasis lesions were identified, of which 286 were detectable on PET-CT. Univariate and multivariate logistic regression analyses were used to identify independent predictors of PET-CT positivity.

Results: Out of all patients, 86.6% were male and the mean \pm SD age was 64.8 \pm 9.3. Comorbidities were present in 205 patients (46.7%), with chronic obstructive pulmonary disease (COPD) being the most prevalent (27.1%). The majority of metastases were located in the frontal lobe (37.2%) followed by the parietal lobe (26.6%). Notably, PET-CT negative

lesions were more likely to have peritumoral edema than PET-CT positive lesions had (67% vs. 56%, $p=0.004$). The median tumor diameter for PET-CT positive lesions was larger than PET-CT negative lesions (18 vs 10 mm, $p<0.001$). The discriminative accuracy of tumor diameter in predicting PET-CT positivity was found to be high, with an area under the curve (AUC) of 0.70 (95% CI: 0.65 to 0.73). For an optimal cut-off value of 14 mm, sensitivity of tumor diameter was 71.68% and specificity was 58.71%

Conclusion: Brain metastases larger than 14 mm and those without peritumoral edema tend to have increased detectability with PET-CT in a large group of lung cancer patients. Since the diagnostic role of PET-CT could not be fully analyzed due to the study design, further research including patients without brain metastases is recommended.

Keywords: Brain metastasis, lung cancer, magnetic resonance imaging, positron emission tomography - computed tomography

Cite this article as: Yakışık Ç, Satıcı C, Sökücü SN, Erinç A, Akyel R, Aydın Ş. Characteristics of Brain Metastases Identified by PET-CT Imaging in Patients with Lung Cancer. Arch Neuropsychiatry 2026;63:158–162. doi: 10.29399/npa.28938

INTRODUCTION

Brain metastases among patients with lung cancer represent a critical aspect in the management and prognosis of cancer patients, significantly impacting both treatment strategies and follow-up protocols (1). The detection and accurate assessment of brain metastases are essential for guiding therapeutic decisions and improving patient outcomes. These metastases can alter the course of treatment, necessitating specific interventions that can extend survival and enhance the quality of life for patients.

Despite the critical nature of detecting brain metastases, there are significant limitations in the current diagnostic approaches. Magnetic resonance imaging (MRI), although considered the gold standard for detecting brain metastases, is not always feasible for every patient. Various factors such as allergy to contrast agents, metal implants, and patient intolerance due to claustrophobia can limit its use (2). In view of these challenges, there is a need for alternative diagnostic modalities that can reliably identify brain metastases, particularly in cases where MRI screening is not practical or possible (3).

Highlights

- Brain metastases larger than 14 mm are more likely to be detected by PET-CT.
- PET-CT is less effective for brain metastases with peritumoral edema.
- Frontal lobe is the most common site for metastases in lung cancer patients.
- The diagnostic role of PET-CT in brain metastases requires further research.

Positron emission tomography - computed tomography (PET-CT) might be a valuable tool in detecting brain metastases in patients who cannot undergo MRI. Studies have indicated that fluorodeoxyglucose (FDG) PET-CT can detect brain metastases among patients with lung

Correspondence Address: Ayşegül Erinc, University of Health Sciences, Yedikule Chest Diseases and Thoracic Surgery Training and Research Hospital, Department of Pulmonology, İstanbul, Türkiye •

E-mail: draysgul@hotmail.com

Received: 17.09.2024, **Accepted:** 09.12.2024, **Available Online Date:** 02.02.2026

©Copyright 2024 by Turkish Association of Neuropsychiatry - Available online at www.noropsikiyatriarsivi.com

cancer with a sensitivity of approximately 21%, and a specificity of 100%, although this can vary depending on factors such as lesion size and metabolic activity (4). It is believed that recent advances in PET-CT imaging, such as the development of new radiotracers, may further increase its sensitivity and specificity in detecting brain metastases. (5). Moreover, PET-CT can provide metabolic insights that complements the anatomical details obtained from MRI, offering a more comprehensive assessment (6).

Current literature also suggests that PET-CT provides valuable information in the management of brain metastases, such as monitoring treatment response and detecting recurrence, which can be critical for tailoring ongoing therapeutic strategies (7). However, there is a lack of information regarding the specific lesions for which PET-CT might be utilized in follow-up (8).

In this study, we aimed to demonstrate the characteristics of brain metastases that could be diagnosed with PET-CT among patients with lung cancer.

METHODS

Study Design and Setting

We performed a cross-sectional study at Yedikule Chest Diseases and Thoracic Surgery Training and Research Hospital, University of Health Sciences, Istanbul, Türkiye. Our study was conducted in line with the Declaration of Helsinki. The local institutional ethics committee approved the study protocol (ethics approval number: 23/400) and waived the requirement for written informed consent.

Study Population

In this study, we consecutively included 439 patients diagnosed with lung cancer and presenting with brain metastasis. A total of 642 brain metastasis lesions were identified, of which 286 were detectable on PET-CT between 2019 (Date of use of PET-CT in our hospital) and 2023. Lung cancer diagnosis was confirmed histopathologically and brain metastases were detected with contrast-enhanced cranial MRI.

Data Collection

Demographic characteristics, comorbidities, mortality data and survival time were collected from electronic medical records. Imaging data, including the presence of peritumoral edema, location, tumor diameter, brain shift and maximum standardized uptake value (SUVmax) of brain metastases were also recorded.

Definitions and Measurements

All patients underwent GE-Discovery IQ PET CT scan. Patients were instructed to fast for at least six hours before the scan. [¹⁸F] Fluorodeoxyglucose (FDG) was administered intravenously at a dose of 3–5 MBq/kg body weight. Imaging was performed approximately 60 minutes after FDG administration.

Computed tomography scans were obtained for attenuation correction and anatomical localization, followed by PET scans. The PET images were reconstructed using an ordered-subset expectation maximization algorithm. Peritumoral brain edema was defined as the presence of hyperintense signals surrounding the metastatic lesion on T2-weighted MRI sequences, indicating fluid accumulation and associated inflammatory response in the adjacent brain tissue (9).

Cranial diameter was measured as the largest axial dimension of the metastatic lesion on contrast-enhanced T1-weighted MRI sequences, ensuring accurate delineation of tumor boundaries.

Positron emission tomography positivity was assessed using FDG uptake measured by SUV. It is crucial to note that PET positivity in this study did not rely solely on SUVmax. Instead, it also included clinical interpretation by a nuclear medicine specialist, who considered areas of suspected metastasis based on FDG uptake patterns in conjunction with anatomical imaging from CT. This comprehensive approach ensured that PET positivity accurately reflected potential metastatic lesions, integrating both quantitative SUV measurements and qualitative clinical expertise (10).

According to the 9th edition of the TNM classification for lung cancer staging, tumors measuring ≤ 3 cm are classified as T1, those >3 cm and ≤ 5 cm as T2, those >5 cm and ≤ 7 cm as T3, and tumors >7 cm as T4. Regarding lymph node involvement, cases without lymph node involvement are classified as N0; involvement of ipsilateral peribronchial and/or hilar nodes and intrapulmonary nodes is classified as N1; involvement of ipsilateral mediastinal and/or subcarinal nodes is classified as N2; and involvement of contralateral mediastinal and/or hilar nodes, or ipsilateral/contralateral scalene or supraclavicular nodes, is classified as N3. As for M staging, the classification is as follows: tumor presence in the contralateral lung, pleural or pericardial nodules, or malignant effusion is staged as M1a; single extrathoracic metastases within a single organ system are staged as M1b; and M1c is further divided into M1c1, referring to multiple extrathoracic metastases within a single organ system, and M1c2, referring to multiple extrathoracic metastases across multiple organ systems (11).

Data Analysis and Statistical Methods

We used descriptive statistics to define variables. Categorical data were reported as proportions and counts, and continuous data were presented as medians and interquartile ranges (IQR) unless the data were normally distributed. Categorical variables were compared using the chi-square test, and continuous variables were analyzed using the student t-test. Univariate and multivariate logistic regression analyses were performed to identify independent predictors of PET-CT positivity. A receiver operating characteristic (ROC) analysis was performed to identify the diagnostic role and the optimal cut-off value of the continuous independent predictors. The sensitivity, specificity, positive predictive value (PPV), and negative predictive value (NPV) of tumor diameter were calculated using standard two-by-two tables. p-value of <0.05 was considered statistically significant. The analyses were carried out using IBM Statistical Package for Social Sciences (SPSS) Program version 25.

RESULTS

In this study, we evaluated 439 patients diagnosed with lung cancer and presenting with cranial metastasis, of whom 86.6% were male. The mean \pm SD age was 64.8 ± 9.3 . All patients were confirmed to have brain metastases via contrast-enhanced cranial MRI. Comorbidities were present in 205 patients (46.7%), with chronic obstructive pulmonary disease (COPD) being the most prevalent (27.1%), followed by hypertension (HT) at 16.4%, ischemic heart disease (IHD) at 10.5%, and diabetes mellitus (DM) at 10%. Tumor staging revealed that 186 patients (42.4%) had a T4 tumor, while 222 patients (50.6%) had an N3 tumor. Furthermore, 68 patients (15.5%) presented with M1b disease, 70 patients (15.9%) with M1c1 disease, and 301 patients (68.6%) with M1c2 disease. According to the 9th edition of the lung cancer staging system, 371 patients (84.5%) were classified with stage 4B disease, and 67 patients (15.3%) with stage 4A disease. Regarding tumor histology, 175 patients (39.9%) had lung adenocarcinoma, 100 patients (22.8%) had not otherwise specified lung cancer (NOS), 82 patients (18.7%) had small cell lung cancer, 77 patients (17.5%) had squamous cell lung cancer, and 2 patients (0.5%) had large cell lung cancer. Of the total cohort, 400 patients (91.1%) experienced mortality, with a median survival time of 294 days (Table 1).

Table 1. Demographic and clinical characteristics of all patients

Variable	Value
Male sex, n (%)	380 (86.6)
Age (years) (mean ± SD)	64.8±9.3
Comorbidities, n (%)	
DM	44 (10)
HT	72 (16.4)
CHF	24 (5.5)
IHD	46 (10.5)
CRF	9 (2.1)
COPD	119 (27.1)
CVD	4 (0.9)
T Stage, n (%)	
T1	47 (10.7)
T2	81 (18.5)
T3	123 (28)
T4	186 (42.4)
N Stage, n (%)	
N0	54 (12.3)
N1	22 (5)
N2	140 (31.9)
N3	222 (50.6)
M Stage, n (%)	
M1b	68 (15.5)
M1c1	70 (15.9)
M1c2	301 (68.6)
Stage, n (%)	
Stage 4A	67 (15.3)
Stage 4B	371 (84.5)
Shift, n (%)	5 (1.1)
Tumor subtype, n (%)	
NOS	100 (22.8)
Adenocarcinoma	175 (39.9)
Squamous cell carcinoma	77 (17.5)
Large cell carcinoma	2 (0.5)
Small cell carcinoma	82 (18.7)
Lesion, n (%)	
PET (+)	286 (44.5)
PET (-)	356 (55.5)
Mortality, n (%)	400 (91.1)
Survival (days), median (IQR)	294 (90-505)

CHF: congestive heart failure; COPD: chronic obstructive pulmonary disease; CRF: chronic renal failure; CVD: cerebro-vascular disease; DM: diabetes mellitus; HT: hypertension; IHD: ischemic heart disease; T stage: tumor stage; N stage: node stage; M stage: metastasis stage; NOS: not otherwise specified.

A total of 642 brain metastasis lesions were identified, of which 286 were detectable on PET-CT. Among the lesions visible on PET-CT, 124 (43%) were classified as adenocarcinoma, 73 (26%) as NOS, 50 (17%) as small cell carcinoma, 37 (13%) as squamous cell carcinoma, and 1 (0.003%) as large cell carcinoma. The majority of metastases were located in the frontal lobe (37.2%) and the parietal lobe (26.6%). Notably, PET-CT negative lesions were more likely to have peritumoral edema than PET-CT positive lesions had (67% vs. 56%, p=0.004). The median tumor diameter for PET-CT positive lesions was larger than PET-CT negative lesions (18 vs 10 mm, p<0.001). There were no significant differences in terms of age, gender, comorbidities, the tumor subtype, the localization of the metastasis, survival and the mortality rates (p>0.05) (Table 2).

Table 2. Lesion-based comparison of the groups

Variable	PET (+) (n=286)	PET (-) (n=356)	p value
Male sex, n (%)	246 (86)	311 (87)	0.64
Age (years) (mean ± SD)	65±9.4	65.1±9.6	0.76
Comorbidities, n (%)			
DM	33 (11)	27 (10)	0.10
HT	51 (17)	53 (15)	0.33
CHF	12 (6)	20 (4)	0.46
IHD	27 (9)	35 (10)	0.89
CRF	2 (1)	11 (3)	0.03
COPD	81 (28)	90 (25)	0.41
Tumor diameter (mm), median (IQR)	18 (12-26)	10 (7-17)	<0.001
Peritumoral edema, n (%)	159 (56)	238 (67)	0.004
Tumor subtype, n (%)			0.71
NOS	73 (26)	69 (19)	
Adenocarcinoma	124 (43)	138 (39)	
Squamous cell carcinoma	37 (13)	69 (19)	
Large cell carcinoma	1 (0.003)	1 (0.002)	
Small cell carcinoma	50 (17)	77 (21)	
Tumor localization, n (%)			0.15
Supratentorial	227 (79.4)	265 (74.4)	
Frontal	84 (29.4)	96 (27)	0.38
Parietal	76 (26.6)	91 (25.6)	0.38
Oksipital	34 (11.9)	44 (12.4)	0.38
Temporal	33 (11.5)	34 (9.6)	0.38
Infratentorial	59 (20.6)	91 (25.6)	
Cerebellum	55 (19.2)	82 (23)	0.38
Mesencephalon	0 (0)	6 (1.7)	0.38
Pons	3 (1)	2 (0.6)	0.38
Bulbus	1 (0.3)	1 (0.3)	0.38
Survival (days), median (IQR)	240.5 (83-415)	278 (112-470)	0.96
Mortality, n (%)	261 (91)	337 (95)	0.11

CHF: congestive heart failure; COPD: chronic obstructive pulmonary disease; CRF: chronic renal failure; CVD: cerebrovascular disease; DM: diabetes mellitus; HT: hypertension; IHD: ischemic heart disease; NOS: not otherwise specified.

Multivariate logistic regression analysis was performed to identify independent predictors of PET-CT positivity. Tumor diameter (OR: 1.05, 95% CI 1.03-1.06; p <0.001) and peritumoral edema (OR: 0.50, 95% CI 0.35-0.72; p <0.001) were found to be independent predictors of PET-CT positivity of the cranial metastases (Table 3).

Table 3. Multivariate logistic regression analyses for independent predictors of PET positive cranial metastasis

Variable	OR	CI (95%)	p value
Peritumoral edema	0.50	0.35-0.72	<0.001
Tumor diameter	1.05	1.03-1.06	<0.001

CI: confidence interval; OR: odds ratio.

The discriminative accuracy of tumor diameter in predicting PET-CT positivity was found to be high, with an area under the curve (AUC) of 0.70 (95% CI: 0.65 to 0.73) (Fig. 1). An optimal cut-off value was calculated as 14. Following categorizing the patients with this cut-off value, two-by-two table analysis revealed that the sensitivity of tumor diameter was 71.68% (95% CI: 65.08% to 76.83%), and the specificity was 58.71% (95% CI: 53.40% to 63.87%) (Table 4).

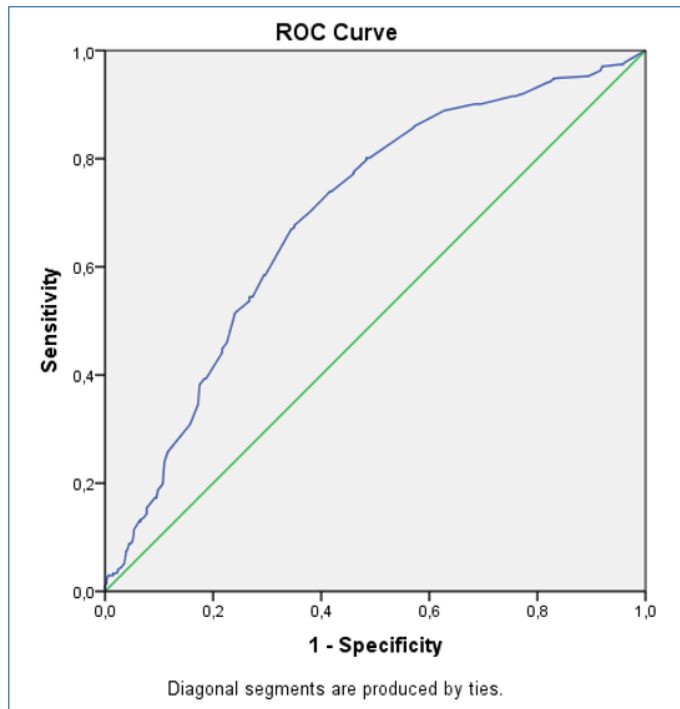


Figure 1. ROC curve of tumor diameter in predicting PET-CT positivity: the ROC curve illustrates the predictive accuracy of tumor diameter for PET-CT positivity in brain metastases among lung cancer patients. The area under the curve (AUC) is 0.70 (95% CI: 0.65–0.73), indicating moderate discriminative power with an optimal cut-off value of 14 mm for tumor diameter, achieving a sensitivity of 71.68% and specificity of 58.71%.

Table 4. Discriminative accuracy of tumor diameter in predicting PET positivity

Parameter*	Value	95% CI
Sensitivity (%)	71.68	65.08 to 76.83
Specificity (%)	58.71	53.40 to 63.87
Positive likelihood ratio	1.74	1.50 to 2.00
Negative likelihood ratio	0.48	0.39 to 0.59
Disease prevalence (%)	44.55	40.66 to 48.49
Positive predictive value (%)	58.24	54.71 to 61.69
Negative predictive value (%)	72.07	67.79 to 75.98
Accuracy (%)	64.49	60.65 to 68.19
AUC (%)	0.70	0.65 to 0.73

* Tumor diameter ≥ 14 mm vs < 14 mm; AUC: area under curve; CI: confidence interval.

DISCUSSION

In this study, we aimed to evaluate the utility of PET-CT in detecting brain metastases among patients with lung cancer. Our findings suggest that PET-CT might be helpful in identifying brain metastases in patients who are unable to undergo contrast-enhanced MRI. PET-CT could detect

particularly larger brain metastasis (≥ 14 mm), while the presence of peritumoral edema actually decreased the detectability of these lesions.

Positron emission tomography - computed tomography is effective in identifying malignant lesions larger than 6 mm, while lesions smaller than 6 mm may result in false negative results (12). However, in the context of brain metastasis, the detectable size threshold on PET-CT tends to be higher (13). It has been demonstrated that as the size of brain metastases increases, the detectability on PET/CT also improves (14). Nevertheless, the exact size at which brain metastases become reliably detectable by PET/CT remains unclear. Our study demonstrates that in lung cancer patients, brain metastases larger than 14 mm are more likely to be detected by PET/CT, highlighting the critical role of lesion size in diagnostic accuracy. This finding aligns with previous research, which demonstrated that PET/CT's effectiveness increases significantly for lesions above 10 mm (15). However, it's important to note that different tumor types may exhibit varying levels of FDG uptake in brain metastases. Unlike studies that included brain metastases from various primary tumors, our research specifically focused on patients with lung cancer, thereby providing more targeted insights into PET/CT's performance in this patient population.

The presence of peritumoral edema, which we found to decrease the detectability of brain metastases on PET-CT, has been supported by similar findings in the literature (16). The impact of peritumoral edema on PET-CT depends on the size of the edema and the characteristics of the tumor (17). During the detection of brain metastases, peritumoral edema generally reduces FDG uptake, which can negatively affect PET-CT's ability to detect metastases (18). Peritumoral edema is commonly observed in deeply located tumors, which are typically associated with a greater degree of edema (19). Therefore, it is important to recognize the increased likelihood of edema in such deeply situated lesions, and to approach the interpretation of PET/CT findings in these patients with heightened caution. However, when peritumoral edema is absent, PET-CT indicated an increased effectiveness in accurately detecting tumors, making it a valuable tool in the diagnosis and management of brain metastases. This highlights the potential of PET-CT as a powerful imaging modality, especially in cases where the tumor is well-defined and not obscured by surrounding edema.

Our findings indicate that neither the subtype of lung cancer nor the tumor localization of brain metastases had a significant impact on PET-CT uptake. This study is consistent with studies that also found that FDG uptake in brain metastases is largely independent of the primary tumor subtype and specific location within the brain (20). Conversely, other studies have suggested that certain histological subtypes of lung cancer, like small-cell lung carcinoma, may demonstrate slightly higher uptake on PET-CT compared to non-small cell lung carcinoma, yet these differences do not translate into clinical significance for detection rates (21,22).

Our study has certain limitations, including its single-center design and retrospective nature. The evaluation of brain metastases on PET-CT was conducted by a single nuclear medicine physician, which may introduce an element of subjectivity. Furthermore, all patients included in the study had brain metastases confirmed by contrast-enhanced MRI, and those without metastases were excluded. Consequently, we were unable to assess diagnostic parameters such as sensitivity and specificity for PET-CT in detecting brain metastases. While our findings provide baseline data on the types of metastases that PET-CT can detect, further studies are needed to evaluate the diagnostic power of PET-CT more comprehensively. Despite these limitations, our study included a substantial number of brain metastases cases within a large group of patients, offering valuable insights into the utility of PET-CT in this context.

We concluded that brain metastases larger than 14 mm and those without peritumoral edema tend to have increased detectability with PET-CT in a large group of lung cancer patients. Since the diagnostic role of PET-CT could not be fully analyzed due to the study design, further research including patients without brain metastases is recommended.

Ethics Committee Approval: The study was a cross-sectional study conducted at Yedikule Chest Diseases and Thoracic Surgery Training and Research Hospital, University of Health Sciences, and was conducted in accordance with the Declaration of Helsinki. The local institutional ethics committee approved the study protocol (ethical approval number: 23/400).

Informed Consent: Written informed consent is not required.

Peer-review: Externally peer-reviewed.

Author Contributions: Concept- CS, SNS; Design- CS, ÇY; Supervision- CS, ÇY; Resource- ÇY, AE; Materials- ÇY; Data Collection and/or Processing- ÇY, AE; Analysis and/or Interpretation- CS, ŞA; Literature Search- CS, AE; Writing- CS, ÇY; Critical Reviews- CS, RA, SNS.

Conflict of Interest: The authors declared that there is no conflict of interest.

Financial Disclosure: None.

REFERENCES

- Suh JH, Kotecha R, Chao ST, Ahluwalia MS, Sahgal A, Chang EL. Current approaches to the management of brain metastases. *Nat Rev Clin Oncol*. 2020;17:279-299. [\[Crossref\]](#)
- Delmaire C, Savatovsky J, Boulanger T, Dhermain F, Le Rhun E, Métellus P, et al. Imagerie des métastases cérébrales [brain metastases imaging]. *Cancer Radiother*. 2015;19:16-19. [\[Crossref\]](#)
- Terakawa Y, Tsuyuguchi N, Iwai Y, Yamanaka K, Higashiyama S, Takami T, et al. Diagnostic accuracy of ¹¹C-methionine PET for differentiation of recurrent brain tumors from radiation necrosis after radiotherapy. *J Nucl Med*. 2008;49:694-699. [\[Crossref\]](#)
- Li Y, Jin G, Su D. Comparison of gadolinium-enhanced MRI and ¹⁸F-FDG PET/PET-CT for the diagnosis of brain metastases in lung cancer patients: a meta-analysis of 5 prospective studies. *Oncotarget*. 2017;8:35743-35749. [\[Crossref\]](#)
- von Schulthess GK, Steinert HC, Hany TF. Integrated PET/CT. Current applications and future directions. *Radiology*. 2006;238:405-422. [\[Crossref\]](#)
- Silva Santana L, Borges Camargo Diniz J, Mothé Glicho Gasparri L, Buccaran Canto A, Batista Dos Reis S, Santana Neville Ribeiro I, et al. Application of machine learning for classification of brain tumors: a systematic review and meta-analysis. *World Neurosurg*. 2024;186:204-218.e2. [\[Crossref\]](#)
- Eude F, Guisier F, Salaün M, Thiberville L, Pressat-Laffouilhère T, Vera P, et al. Prognostic value of total tumour volume, adding necrosis to metabolic tumour volume, in advanced or metastatic non-small cell lung cancer treated with first-line pembrolizumab. *Ann Nucl Med*. 2022;36:224-234. [\[Crossref\]](#)
- Damle NA, Bal C, Bandopadhyaya GP, Kumar L, Kumar P, Malhotra A, et al. The role of ¹⁸F-fluoride PET-CT in the detection of bone metastases in patients with breast, lung and prostate carcinoma: a comparison with FDG PET/CT and ^{99m}Tc-MDP bone scan. *Jpn J Radiol*. 2013;31:262-269. [\[Crossref\]](#)
- Laajava J, Korja M. Peritumoral T2/FLAIR hyperintense MRI findings of meningiomas are not necessarily edema and may persist permanently: a systematic review. *Neurosurg Rev*. 2023;46:193. [\[Crossref\]](#)
- Joseph S, Singh E. Nuclear medicine PET/CT breast cancer assessment, protocols, and interpretation. *StatPearls* [Internet]. 2023 Apr 3. Treasure Island (FL): StatPearls Publishing; 2024.
- Li HY, Wang YY, Liu H, Liu HX, Jiang LY, Han YC, et al. The ninth edition of TNM staging for lung cancer: precise staging for precise diagnosis and treatment. *Zhonghua Wai Ke Za Zhi*. 2024;62:537-542. [\[Crossref\]](#)
- Boellaard R, O'Doherty MJ, Weber WA, Mottaghy FM, Lonsdale MN, Stroobants SG, et al. FDG PET and PET/CT. EANM procedure guidelines for tumour PET imaging, version 1.0. *Eur J Nucl Med Mol Imaging*. 2010;37:181-200. [\[Crossref\]](#)
- Wu Y, Li P, Zhang H, Shi Y, Wu H, Zhang J, et al. Diagnostic value of fluorine ¹⁸ fluorodeoxyglucose positron emission tomography/computed tomography for the detection of metastases in non-small-cell lung cancer patients. *Int J Cancer*. 2013;132:E37-E47. [\[Crossref\]](#)
- Xu T, Zhang X, Zhang S, Liu C, Fu W, Zeng C, et al. Imaging features and prognostic value of ¹⁸F-FDG PET/CT detection of soft-tissue metastasis from lung cancer: a retrospective study. *BMC Cancer*. 2020;20:596. [\[Crossref\]](#)
- Kitajima K, Nakamoto Y, Okizuka H, Onishi Y, Senda M, Suganuma N, et al. Accuracy of whole-body FDG-PET/CT for detecting brain metastases from non-central nervous system tumors. *Ann Nucl Med*. 2008;22:595-602. [\[Crossref\]](#)
- Ling X, Xu H. PET/CT of metastatic tumors. In: Yao Z, Li S, editors. *Atlas of PET/CT in Oncology*, Vol. 1: Brain, Head and Neck Cancers. Singapore: Springer; 2023. [\[Crossref\]](#)
- Frati A, Armocida D, Arcidiacono UA, Pesce A, D'Andrea G, Cofano F, et al. Peritumoral brain edema in relation to tumor size is a variable that influences the risk of recurrence in intracranial meningiomas. *Tomography*. 2022;8:1987-1996. [\[Crossref\]](#)
- Li D, Zhang J, Ji N, Zhao X, Zheng K, Qiao Z, et al. Combined ⁶⁸Ga-NOTA-PRGD2 and ¹⁸F-FDG PET/CT can discriminate uncommon meningioma mimicking high-grade glioma. *Clin Nucl Med*. 2018;43:648-654. [\[Crossref\]](#)
- Zidan MA, Hassan RS, El-Noueam KI, Zakaria YM. Brain metastases assessment by FDG-PET/CT. Can it eliminate the necessity for dedicated brain imaging? *Egypt J Radiol Nucl Med*. 2020;51:223. [\[Crossref\]](#)
- Özütemiz C, Neil EC, Tanwar M, Rubin NT, Ozturk K, Cayci Z. The role of dual-phase FDG PET/CT in the diagnosis and follow-up of brain tumors. *AJR Am J Roentgenol*. 2020;215:985-996. [\[Crossref\]](#)
- Fletcher JW, Djulbegovic B, Soares HP, Siegel BA, Lowe VJ, Lyman GH, et al. Recommendations on the use of ¹⁸F-FDG PET in oncology. *J Nucl Med*. 2008;49:480-508. [\[Crossref\]](#)
- Fletcher JW, Kymes SM, Gould M, Alazraki N, Coleman RE, Lowe VJ, et al. A comparison of the diagnostic accuracy of ¹⁸F-FDG PET and CT in the characterization of solitary pulmonary nodules. *J Nucl Med*. 2008;49:179-185. [\[Crossref\]](#)